Proceeding *20th SEAGC - 3rd AGSSEA Conference in conjunction with 22nd Annual Indonesian National Conference on Geotechnical Engineering.* Jakarta - INDONESIA, 6 -7 November 2018. ISBN No. 978-602-17221-6-9

Stability Analysis of an Overall Failure Excavation Case in Hang Zhou

T. N. Do[1]
[1]*Department of Civil Engineering, Thuyloi University, Hanoi, Vietnam*
E-mail: dotuannghia@tlu.edu.vn

ABSTRACT: In this paper, stability of an overall failure excavation case in Hang Zhou, China was analyzed using the finite element method (FEM). The retaining system of the excavation was fully modelled, including walls, horizontal struts, and vertical center posts. For comparison, the structural elements were simulated using plates with both elastic and elastoplastic behaviors. The soil response nesar failure was assumed to follow the Morh-Coulomb model. Results showed that the FEM using the elastoplastic retaining system gave a more reasonable estimate of stability of the excavation than that using the elastic support system. With the elastoplastic retaining system, yielding firstly occurred on the wall and then on the struts, which caused large movement of surrounding soil toward the excavation. On the other hand, with the elastic retaining system, failure of the excavation was only due to the great plastic heave of soil at the excavation bottom. The predicted movement of soil and wall was nearly one meter as using the ealstoplatic support system but several meters as using the elastic one.
Keywords: Deep excavations, stability analysis, finite element method, failure mechanism.

1. INTRODUCTION

Stability of deep excavations is one of the main concerns of practical engineers. Failure of excavations is often characterized by collapse of the support system and the large inward movement of surrounding soil. Therefore, occurrence of failure would result in not only economic losses (e.g., destruction of neighboring facilities) but also casualties. Most recently, a 15.7-m-deep excavation in Hangzhou, China, collapsed because the lowest strut level was not installed timely, causing twenty one casualties. Based on an intensive investigation, Chen et al. (2013) predicted the failure surface of soil from the disturbance of surrounding soil.

Stability problem of excavations has been studied by many researchers using the FEM with reduced shear strength. A parametric study by Goh (1990) showed that the factor of safety would be increased with the embedded depth and the stiffness of the wall but reduced with the thickness of the clay layer below the excavation bottom. Faheem et al. (2003) also performed a parametric study and gave consistent results with those by Goh (1990). Furthermore, closed form equations considering the wall embedded depth were developed to estimate the bearing capacity factor (N_c). Based on case studies, Do et al. (2013) showed that the strength reduction ratio (SR) of soil, corresponding to the onset of rapid development of the nodal displacement, was able to represent the factor of safety of excavations. For convenience, most of previous studies employed the elastic support system and did not model the existence of center posts used to support the horizontal struts, so that the finite element model might not simulate sufficiently behaviors of excavations in the site. In addition, few researchers address to failure mechanism of excavations in soft clay, which is strongly affected by the subsoil profile (e.g. existence of hard stratum) and stiffness of the support system, so that this problem remains to be resolved.

In this study, the FEM with reduced shear strength was used to investigate failure mechanism of the Hangzhou case. Details of the strength reduction technique can be seen elsewhere (e.g., Do et al., 2013). Center posts were considered in the finite element model. For comparison, both the elastic and elastoplastic support systems were employed.

2. HANGZHOU CASE

2.1 Ground Conditions and Construction Sequence

The Hangzhou case was a 21.2- × 107.8-m internally braced excavation, which was a part of an underground subway station. The construction sequence and subsurface conditions of the case are plotted in Fig. 1. The excavation had a maximum depth of 15.7 m and was performed in five stages. The support system was composed of a 0.8-m-thick and 33-m-deep diaphragm wall and four steel pipe strut layers at GL -0.5 m, -4.2 m, -8.5 m, and -12.4 m with horizontal spacing of 2.9 m. Center posts were embedded into 0.8-m-diameter bored piles. The site stratigraphy consists of eight subsoil layers, at which most of them are soft clay, ranging from GL -2.0 m to -50.0 m. The undrained shear strength of soil obtained from field Vane shear test at two boring holes (V01 and V07) (Chen et al., 2013) are also included in the figure. The ground water table is located at GL -2.0 m. As shown in Fig. 2, when collapse of excavation occurred, the wall had a deep inward deformation and was broken into two parts. Connections between struts and walls were failed and center posts were tilted toward the right wall. The soil heave at the excavation bottom was 2.5 m and the subsidence of the adjacent road was 7 m (Chen et al., 2013).

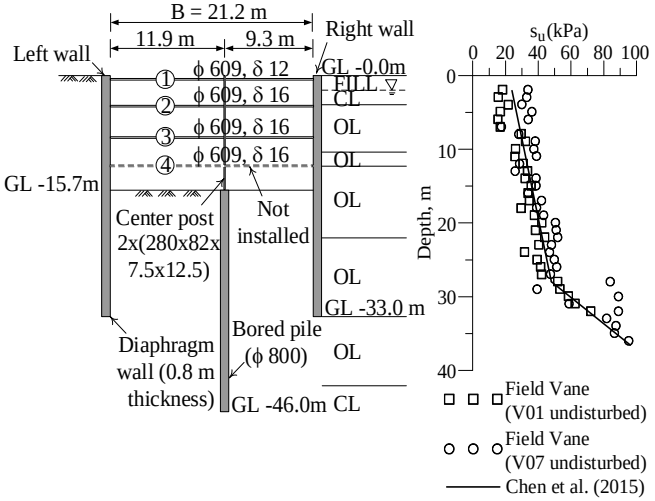

Figure 1 Construction sequence and subsurface conditions

Figure 2 Failure of excavation

2.2 FE Analysis

Since most of the subsoil is saturated clay, it was assumed that the behavior of soil is elastoplastic and well-described by the Mohr-Coulomb model. The model requires five input parameters, including Young's modulus (E), Poisson's ratio (ν), friction angle (ϕ), cohesion (c), and dilatancy angle (ψ). Clayey soils were simulated as undrained materials, at which $\nu_u = 0.495$, $\phi_u = 0^0$, c_u = su, and Eu = 450su. su was taken from the average results of Vane shear tests.

The structural elements (struts, walls, and center posts) were modeled using plate elements, which required four input parameters including axial stiffness (EA), flexural rigidity (EI), maximum (plastic) bending moment (Mp), and maximum (plastic) axial force (Np). The input parameters of the elastoplastic structural elements used for analysis were listed in Table 1. When the elastic structural elements were employed, the Mp and Np values would be very high, e.g., Mp = 1015 kNm and Np = 1015 kN (per meter width). For the reinforced concrete wall at this case, the compressive strength of concrete (fc') was assumed to be 21 MPa. The Young's modulus (E) was equal to 15000(fc')0.5. The Mp value was calculated using a cross section analysis program, namely XTRACT, from wall thickness, area of steel reinforcement, and properties of concrete and steel. The N_p value was estimated according to ACI 318-11. Since the wall may have cracks due to bending during excavation and the quality of concrete of the wall cast in stabilizing fluid properly does not meet the design requirements, a reduction factor of 0.8 was applied to the input parameters (EA, EI, M_p, and N_p) of the wall. On the other hand, EA, EI, M_p, and N_p of struts were calculated based on the assumption that the Young' s modulus (E) and the yield stress (σ_y) of struts were 2.04×10^8 kN/m2 and 250 MPa, respectively. Due to the improper installation of struts in the field (i.e., they are not totally straight as splicing H steel together), their parameters were reduced by 10%. EA and N_p of center posts were determined similarly to those of struts. EI and M_p of center posts were not considered to avoid any restriction on soil movement below the excavation bottom.

During the strength reduction procedure, the soil strength at the final excavation stage was reduced successively by increasing the SR ratio. The divergence of numerical solutions was defined as the failure of the excavation. The maximum ratio, namely SRmax, at which numerical solutions still converge, was treated as the factor of safety of the excavation. For understanding the percentage of load being applied at the final stage, ΣMstage is defined as the ratio of the load applied successfully in calculation to that caused by excavation at the final stage.

Table 1 Input parameters (per meter width) of structural elements

Strut layer No.	σ_y (MPa)	f_c' (MPa)	EA (kN)	EI (kNm^2)	N_p (kN)	M_p (kNm)
1	250		1.4×10^6	6.4×10^4	1750	256
2 and 3	250		1.9×10^6	8.3×10^4	2310	334
Center post	250		2.4×10^5	0	288	0
Wall		40	1.9×10^7	10^6	24260	1186

When the elastoplastic support system was employed, the final excavation stage was not calculated successfully and the ΣMstage max value was 0.6652. Fig. 3a plots the wall deflection and the soil heave as ΣMstage is increased to 98%, 99%, and 100% of ΣMstage max. It is noted that since center posts stayed closer to the left wall than the right wall, as shown in Fig. 1, the deformation of the left wall was greater than that of the right wall in this analysis. Therefore, only the left wall deflection was presented in Fig. 3a. As shown in Fig. 3a, when ΣMstage increased from 98% to 99% of ΣMstage max, the wall deflection and the soil heave did not develop significantly. But when ΣMstage reached the maximum value, the deformations of soil and wall increased rapidly, up to 800 mm each. The maximum wall deflection developed near the final excavation grade (GL -15.7 m). The maximum soil heave occurred at 4 m away from the left wall.

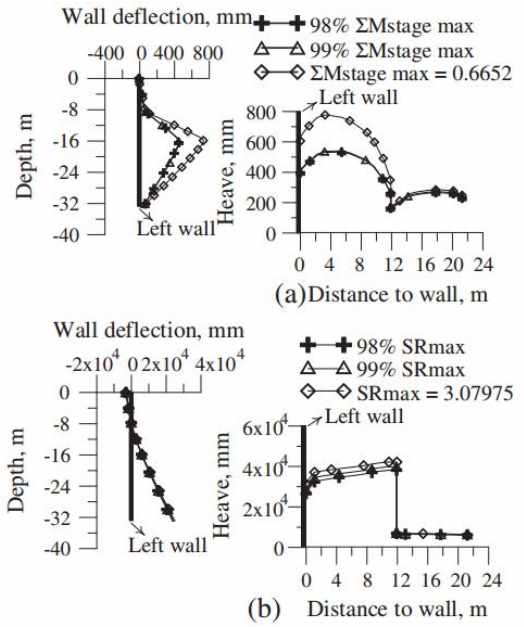

Figure 3 Wall deflection and soil heave as using the elastoplastic (a) and elastic (b) support systems

When the elastic support system was employed, the final excavation stage was computed completely and the SRmax value was 3.07975. The wall deflection and the soil heave corresponding to 98%, 99%, and 100% of SRmax are plotted in Fig. 3b. As shown in the figure, when SR was increased, the wall deflection remained constant and the maximum wall deflection, about 3×104 mm, happened at the wall toe. On the other hand, the soil heave developed gradually with the maximum soil heave occurring at the center of the excavation, up to 4×104 mm. It is observed that the constant wall deflection is due to its elastic behavior whereas the increasing large soil heave indicates the plastic behavior of soil, which then leads to the divergence of numerical solutions.

Fig. 4 shows the interaction diagrams of internal forces (M, N) of struts and walls in the numerical analysis as using the elastoplastic support system. As shown in the figure, when excavation was performed from the 1st stage to the 5th stage (final stage), bending moment had a greater impact than axial load on the behaviors of struts at the 1st and 2nd layers and the wall because

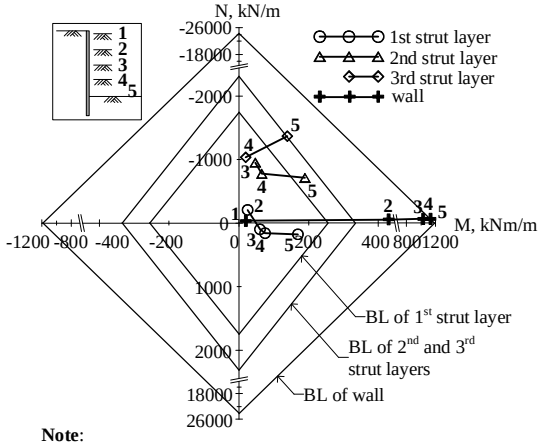

Note:
BL represents boundary lines.
At the 5th stage, internal forces corresponding to ΣMstage max are plotted.

Figure 4 Interaction diagram of internal forces of elastoplastic structural elements

their internal force curves developed along the M axis. On the other hand, since the internal force curve of struts at the 3rd layer grew closer to the N axis than the M axis, their behaviors were strongly affected by axial load. The wall started to yield at the 4th excavation stage, which was earlier than the strut system. At the final stage (ΣMstage max), both the wall and struts at the 3rd layer yielded whereas struts at the 1st and 2nd layers remained elastic behaviors.

Fig. 5a shows the incremental displacements of soil and elastoplastic structural elements at the last calculation step of the final excavation stage corresponding to the ΣMstage max value. As shown in this figure, because of the soil weight, the soil behind the wall moved downward and toward the wall but did not pass below the wall toe. The wall was pushed to deform and yield at the final excavation grade, as marked with a rectangle and a square in the figure. Due to the asymmetric characteristics of the excavation, the left wall yielded more seriously than the right one and had an additional plastic hinge at the 3rd strut level. The inward deformation of the wall mainly caused the soil heave at the excavation bottom. The downward sinking of the wall bent the horizontal struts, as presented in the enlarged area, but the bending effect was not enough to cause yielding of struts at the 1st and 2nd layers. Yielding of struts at the 3rd layer, as marked with a circle, on the other hand, was a result of the large axial load transferred from the wall. It is noted that since center posts were supported by bored piles, which were embedded deeply into subsoil, the upward movement of center posts under the effect of the soil heave was not significant. These observed deformations are in good agreement with those in the site (Fig. 2), at which the wall was broken, struts were destroyed, and center posts were tilted toward the right wall.

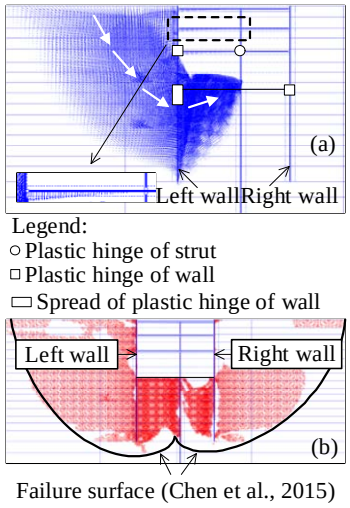

Figure 5 Incremental displacement plot (a) and plastic point plot (b) at ΣMstage max as using the elastoplastic support system

Fig. 5b is the plastic point plot of soil at ΣMstage max as using the elastoplastic support system. It is observed that plastic points of soil distribute in front and back of the wall but do not spread below the wall toe, which is consistent with the soil movement mentioned previously. Also, the distribution of plastic points is in good agreement with the failures surface predicted by Chen et al. (2013) based on the soil investigation after failure of the excavation.

3. CONCLUSION

The following conclusions can be drawn on the basis of the work presented herein:

i. With the numerical analysis of the Hangzhou case, it is found that when the elastoplastic support system is employed, the yielding of struts and walls firstly causes a sudden increase in the wall deflection and the soil heave, and then the failure of the excavation. On the other hand, as using the elastic support system, the failure of the excavation is caused by the large soil plastic heave at the excavation bottom. The amount of the wall deflection and the soil heave obtained in the elastic case, i.e., soil plastic heave, was much higher than that in the elastoplastic case, i.e., failure of structural system, by several orders from the point of view of numerical solutions.

ii. For the Hangzhou case (with an insufficiently installed strut system), the soil behind the wall moved directly toward the wall, pushing the wall to have a bulging deflection and yield. Then, struts yield due to the large axial load transferred from the wall. Yielding of struts and walls leads to the movement of surrounding soil toward the excavation zone.

4. REFERENCES

American Concrete Institute (ACI), (2011) "Building code requirements for structural concrete (ACI 318-11) and Commentary (ACI 318R-11)". Detroit.

Chen R.P., Li Z.C., Chen Y.M., Ou C.Y., Hu Q., and Rao M., (2013) "Failure investigation at a collapsed deep excavation in very sensitive organic soft clay". Perform. Constr. Facil. 04014078.

Do T.N., Ou C.Y., and Lim A., (2013) "Evaluation of factors of safety against basal heave for deep excavations in soft clay using the finite element method". Geotech Geoenviron Eng 2013, 139, pp2125–2135.

Faheem H., Cai F., Ugai K., and Hagiwara T., (2003) "Two-dimensional base stability of excavations in soft soils using FEM". Computer and Geotechnics, 30, Issue 2, pp141–163.

Goh A.T.C., (1990) "Assessment of basal stability for braced excavation systems using the finite element method". Computer and Geotechnics, 10, Issue 4, pp325–338.